Temporal and Spatial Measurements of the Electron Density Perturbation Produced in the Wake of an Ultrashort Laser Pulse

J. R. Marquès,[1] J. P. Geindre,[1] F. Amiranoff,[1] P. Audebert,[1] J. C. Gauthier,[1] A. Antonetti,[2] and G. Grillon[2]
[1]*LULI, Ecole Polytechnique–CNRS, 91128 Palaiseau, France*
[2]*LOA, ENSTA, Ecole Polytechnique–CNRS, 91120 Palaiseau, France*
(Received 30 October 1995)

The plasma electron density oscillation produced in the wake of a narrow (beam waist ≪ plasma wavelength) ultrashort laser pulse is measured for the first time, with a temporal resolution much better than the electron plasma period and a high spatial resolution along the laser focal spot diameter. The relative density perturbation is between 30% and 100%, in good agreement with numerical simulations. [S0031-9007(96)00154-8]

PACS numbers: 52.40.Nk, 52.75.Di

Recently, there has been great interest in the production of large amplitude electron plasma waves (EPW) because of their potential application for particle acceleration [1,2] or photon acceleration [3]. Three main schemes of EPW production have been proposed. In the laser beatwave (LBW) scheme [1], and EPW is resonantly excited by the temporal beating of two relatively long [$\omega_{pe}\tau \gg 1$, where τ is the pulse duration, $\omega_{pe} = (n_e e^2/m_e \varepsilon_0)^{1/2}$ is the electron plasma frequency, e and m_e the electron charge and mass, n_e the electron density, and ε_0 the vacuum permittivity] copropagating laser pulses with angular frequencies ω_1, $\omega_2 \gg \omega_{pe}$. The EPW reaches its maximum amplitude when $\omega_{pe} \cong \omega_1 - \omega_2$. The charge separation associated with the EPW induces a longitudinal electric field with a relativistic phase velocity and an amplitude that can reach tens of GV/m. Such electric fields could be used for particle acceleration to ultrahigh energies. LBW acceleration has been demonstrated in experiments using a CO_2 [4] or a Nd:glass [5] laser. Electric fields in the GV/m range have been measured, and injected electrons have been accelerated with energy gains of several MeV.

In the laser wakefield (LWF) scheme [1,6], the EPW is excited by the ponderomotive force associated with the temporal profile of a short laser pulse. The EPW is maximum when the resonance condition $\omega_{pe}\tau \approx 1$ is satisfied. The LWF process is very attractive because the width of its resonance is much larger than for the LBW.

A more complex scheme is the laser self-resonant wakefield (LSRWF) [7], in which a high-power ultrashort laser pulse propagates in a plasma such that $\omega_{pe}\tau \gg 1$ and $P > P_c$, where P and ω are the laser power and frequency, and $P_c(\mathrm{GW}) = 16.2(\omega/\omega_{pe})^2$ is the relativistic self-focusing critical power. The relativistic self-focusing and the Raman instability modulates the laser pulse temporal envelope in a train of pulses verifying $\omega_{pe}\tau \approx 1$. These pulses excite an EPW that can reach the wave breaking amplitude. In recent experiments [8,9] the acceleration of background electrons by the excited EPW to energies up to a few tens of MeV has been observed. In opposition with the LBW and the LWF, the LSRWF relies on instability mechanisms and is, in principle, more difficult to control.

A few investigators have recently underlined the interest of EPW as photon accelerators [3]. The frequency upshifting of a short laser pulse can be obtained by propagating it in an EPW. In opposition with the particle accelerator, the photon accelerator is not sensitive to the electric field of the EPW but only to the electron density perturbation. In other words, the electron oscillation does not need to be longitudinal but can be transverse.

The electron density perturbation produced by the LWF process has not yet been measured in detail. Hamster *et al.* [10] have observed the LWF resonance with spatially and temporally integrated measurements of the electromagnetic radiation at the plasma frequency. Nakajima *et al.* [9] have injected electrons in the wake of a short laser pulse and measured energy gains up to 13 MeV at the resonant density, but without direct measurement of the electron density perturbation. In this Letter we present the first temporally and spatially resolved measurements of the electron density perturbation produced by the LWF process.

A two-dimensional, nonrelativistic, analytical model of the LWF process has been developed by Gorbunov and Kirsanov [6]. The electron motion is calculated assuming a density perturbation δn small compared to the equilibrium density n_0, fixed ions, and a cylindrical geometry. It is also assumed that the radial and temporal parts of the potential can be separated, which, for a Gaussian beam, is valid if the Rayleigh length $z_R = 2\pi\sigma^2/\lambda$ is much larger than $c\tau$ and σ (σ the laser beam waist at $1/e$ in intensity, λ the laser wavelength). The laser intensity in the vicinity of the focus can then be approximated by

$$I(r,t) = I_{\max} \exp(-r^2/\sigma^2) \exp[-(t - z/c)^2/\tau^2].$$

The electron density perturbation produced in the laser pulse wake is then

 0031-9007/96/76(19)/3566(4)$10.00

$$\delta n/n_0 = (\delta n_z + \delta n_r)/n_0$$
$$= A \exp(-r^2/\sigma^2)[1 + (2c/\omega_{pe}\sigma)^2(1 - r^2/\sigma^2)] \times \sin[\omega_{pe}(t - z/c)], \quad (1)$$

where $A = 20.5P(\mathrm{TW})\,(\lambda/\sigma)^2(\omega_{pe}\tau/2)\exp[-(\omega_{pe}\tau/2)^2]$ is an amplitude factor characterizing the LWF resonance (P is the laser pulse maximum power).

The perturbation is the sum of two contributions. The first one, δn_z, comes from the longitudinal oscillation of the electrons induced by the temporal profile of the laser pulse, while the second one, δn_r, corresponds to the transverse motion induced by the radial profile of the pulse. Their ratio on the laser axis is

$$\delta n_r/\delta n_z(r = 0) = (\lambda_p/\pi\sigma)^2,$$

where $\lambda_p = 2\pi c/\omega_{pe}$. Therefore, the electron motion can be treated as longitudinal when $\sigma \gg \lambda_p$, and transverse when $\sigma \ll \lambda_p$. In this experiment, we measure the oscillation with a diagnostic sensitive to the product δnL, where the interaction length L is of the order of the laser Rayleigh length z_R. Equation (1) indicates that, while the product $\delta n z_R$ is independent of σ for the longitudinal perturbation, it increases as $(\lambda_p/\sigma)^2$ for the transverse perturbation:

$$\delta n_z z_R \propto P\lambda, \quad \text{but } \delta n_r z_R \propto P\lambda(\lambda_p/\sigma)^2 .$$

For a given laser pulse duration, λ_p is fixed by the resonance condition $\omega_{pe}\tau \approx 1$. If the longitudinal wakefield ($\sigma \gg \lambda_p$) is most desirable for particle acceleration, the above expression shows that the transverse plasma oscillation is much easier to measure. For this reason, we have chosen to excite this type of oscillation [$30 \leq (\lambda_p/\pi\sigma)^2 \leq 300$ in our experiment].

The principle of the experiment is the following: A pump beam is focused into a chamber filled with helium gas. It ionizes the gas near the focus and excites the electron perturbation. A double pulse beam is focused on the same axis, and the perturbation is measured by the frequency-domain interferometry technique [11]. If the two probe pulses propagate in the regions of maximum and minimum densities in the wake of the laser pulse (see Fig. 1), they will experience a phase shift which can be measured after a temporal recombination in a spectrometer. The temporal beating creates a system of fringes in the frequency domain. The position of the fringes depends on the relative phase between the two pulses. It should be noted that in this experiment the group velocity of the probe pulses is almost equal to the phase velocity of the EPW, so that the two probe pulses stay in phase with the density maxima and minima during the propagation. At the output of the spectrometer the horizontal axis give the position of the fringes (perturbation amplitude), while the vertical axis gives the one-dimensional spatial resolution.

The experimental setup is shown in Fig. 2. The LOA 10 Hz Ti:sapphire laser beam at a wavelength of 800 nm with a maximum of 40 mJ and a duration of 120 fs (FWHM) is split into two parts. The reflected part (80%) is used as the pump beam, and the transmitted part as the probe beam. This beam is frequency doubled and sent into a Michelson interferometer to generate two colinear pulses with an adjustable time delay. These two pulses pass through an aperture to improve the phase front homogeneity and increase their focal spot diameter to a size much larger than the pump focal spot size. The time delay between the pump and the probe pulses is adjusted with a delay line. The probe beam is put back collinearly with the pump by transmission through a dielectric mirror reflecting the pump. The pump and probe pulses are focused by an $f/8$ MgF_2 lens. The focal spot intensity profiles show that the pump focal spot is almost Gaussian with a radius (at $1/e$) $\sigma = 5.5 \pm 0.5$ μm, while the probe radius is 140 μm. The maximum pump intensity is 2.6×10^{17} W/cm^2, giving a fully ionized helium gas in the focal region [12]. The focal plane is imaged on the spectrometer slit with an $f/2.4$ doublet, giving a magnification of 20 and a spatial resolution of 1.2 μm. The pump beam is attenuated before the imaging lens by an infrared filter. The focal plane is imaged on a charge coupled device camera to control the alignment on the spectrometer slit and the pump-probe spatial overlap. The spectrometer is of the Czerny-Turner type of 1 m focal length and $f/7.5$ aperture. The spectral resolution is 0.3 Å, and the time stretching is 48 ps.

The experimental procedure is the following: For each gas pressure, the time separation of the two probe pulses is adjusted to $1.5T_{pe}$ as shown in Fig. 1 ($T_{pe} = 2\pi/\omega_{pe}$ is the EPW period for a fully ionized helium gas). In this configuration, when one of the probe pulses coincides with a maximum of the density perturbation, the second one is on a minimum. In that case, the phase difference between the two pulses corresponds to the peak-to-peak density perturbation. Two modes of measurements are

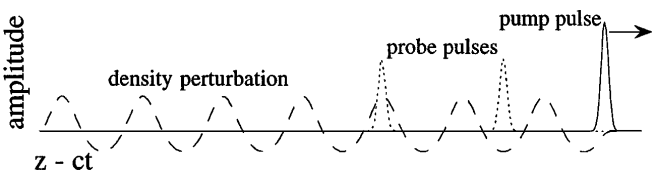

FIG. 1. Principle of the experiment.

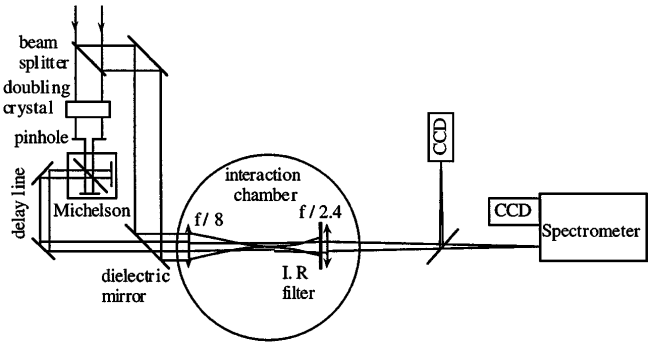

FIG. 2. Experimental setup.

possible [10]. In the absolute mode, the first probe pulse is before the pump (no plasma) and the second one after. The relative phase shift between the pulses arises from the plasma formation and gives us the radial plasma profile. This measurement also gives us the time separation Δt between the pump and the two probe pulses ($\Delta t = 0$ when the second pulse is on the pump maximum, which corresponds to the maximum phase shift). In the relative mode, the two probes are after the pump, so that both travel after the plasma formation. Their relative phase is due to a perturbation produced in the pump pulse wake. By recording the relative phase for different time delays between the probe and pump pulses, one can measure the temporal evolution of the electron perturbation.

Figure 3 presents typical curves of the radial profile of the relative phase. Curve (a) corresponds to a position of the delay line where the phase amplitude is maximum. Curve (c) is the pump focal spot intensity profile. As expected from Eq. (1), the phase transverse profile presents two parts: a central part at $r < \sigma$ ($= 5.5\ \mu$m), and bumps on its sides. The central part comes from the initial transverse expulsion of the electrons located on the laser axis. These electrons are expelled and increase the electron density on both sides of the focus, which is evidenced by the bumps on the phase profile. Curve (b) is obtained half a plasma period later. As expected, it presents a reversed shape. We note that a flat profile (null phase) is measured when we delay the probes to a quarter of a plasma period after an extremum. We have also added in Fig. 3 the transverse profile of the phase obtained in the absolute mode (d). This curve, reduced by a factor of 6, shows the radial plasma profile. Even if the helium gas is 2 times ionized around the focus, the phase profile does not present a step-like shape. This is due to the integration along the laser axis. The spatial extension of this profile is larger than the one obtained in the relative mode, confirming that this last one comes from a perturbation occurring in the proximity of the laser axis, i.e., close to the maximum laser intensity.

The relative phase between the probe pulses depends on the product δnL. It can be calculated by assuming that the density gradient along the laser propagation axis is a step function. With one pulse on a maximum of the density and the other on a minimum, the relative phase is

$$\Delta\phi = 2\pi(L/\lambda_1)\delta n/n_{c1}\,,$$

where λ_1 and n_{c1} are the wavelength and the critical density of the probe pulses. As the transverse perturbation δn_r is proportional to $1/\sigma^4$, it decreases very quickly when we move away from focus. This means that L can be very well approximated to twice the Rayleigh length z_R ($\approx$200 μm in our experiment). Our measurements show a peak-to-peak phase difference $2\Delta\phi \approx 20$ mrad. The density perturbation is of the order of 3×10^{16} cm^{-3}, and the relative perturbation between 30% and 100%. The measured phase is a temporal average of the density gradient in the probe-pulse envelope and a spatial average along the interaction length, so that the real perturbation amplitude should be even higher. A simple calculation made assuming ionization thresholds of 10^5 W/cm^2 for He^{2+} and 5×10^{15} W/cm^2 for He^{2+} [11] indicates that in our conditions the plasma should be one time ionized from $|z| \leq 12z_R$, and two times ionized for $|z| \leq 4z_R$. Assuming a 100% perturbation for $|z| \leq z_R$, the phase amplitude ratio between the absolute and the relative mode measurements should be 4. Our measurements give a ratio between 4 and 6.

Such high relative amplitudes cannot be calculated with the linear model described, and imply numerical simulation. In our conditions, the expected $\delta n_r/\delta n_z$ is between 30 and 300, so we developed a one-dimensional (transverse) Lagrangian bifluid code. The fluid equations are solved in the nonrelativistic case (v_0/c was less then 0.3 in our experiment) and for a cold plasma. In the density range of this experiment ($3 \times 10^{16} \leq n_e \leq 9 \times 10^{16}$ cm^{-3}), the simulations give $10^{16} \leq \delta n \leq 5 \times 10^{17}$ cm^{-3}, in good agreement with our measurements.

Typical measurements of the phase difference on the laser axis versus the time delay between the probe and pump pulses are presented in Fig. 4 for helium pressures of 0.8 mbar (a) and 1 mbar (b). Each point corresponds to the relative phase difference between two measurements separated by half a plasma period. One can see that the phase amplitude is oscillating with a well defined period. The accuracy on the relative temporal position comes from the delay-line translation and is less than 3 fs. The uncertainty in the absolute time is of the order of 60 fs and is the uncertainty on the zero delay time obtained by the absolute measurement (pump and second probe synchronized). The error bars on the phase come from the long time scale laser energy fluctuations (15%) and from the fact that the gas pressure was increasing by about 0.02 mbar during the data acquisition, decreasing the plasma period by about 1% (a small change on the period is not very sensitive on the first oscillations, but dramatically changes the position of later oscillations, spreading the points during the measurements). Accordingly, the numerical

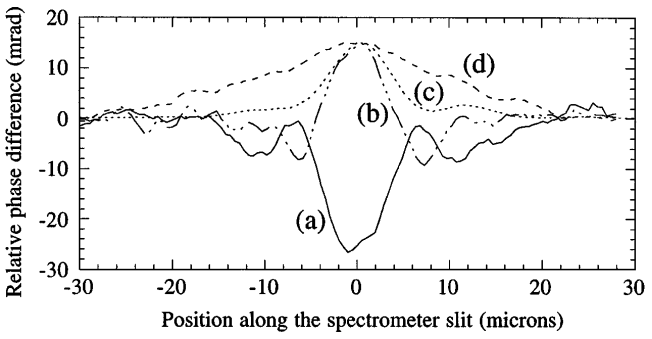

FIG. 3. Radial profile of the relative phase difference. Line (a) corresponds to the phase at a maximum of the perturbation, line (b) is $0.56T_{pe}$ later. Line (c) is the measured pump laser intensity profile, and line (d) is a normalized ionization profile measured in the absolute mode.

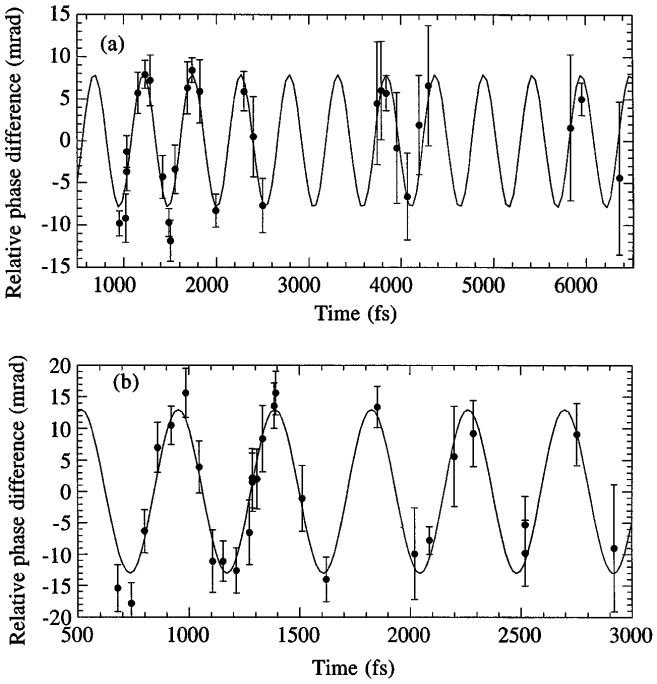

FIG. 4. On-axis relative phase versus time for helium pressures of 0.8 mbar (a) and 1 mbar (b). The points correspond to the experiment and the solid curve to a numerical fit: (a) $7.9\sin[2\pi(\text{time} - 555)/526]$, (b) $13\sin[2\pi(\text{time} - 407)/436]$.

fit (solid line) has been performed on the first plasma oscillations. Even if the density perturbation is nonlinear, the measured phase still has a sinusoidal behavior. This can be due to two main reasons: With a time separation of $1.5T_{pe}$ between the probe pulses, the measured phase corresponds to the peak-to-peak amplitude, and so should present a symmetric behavior near zero. The maxima of a nonlinear density perturbation are very narrow in space and time. The temporal envelope of the probe pulses and the finite spatial resolution of the imaging system average these narrow peaks. Simulations taking into account these effects will be described in a forthcoming publication.

Figure 5 shows the measured oscillation period as a function of the electron density (the helium gas is assumed fully ionized). The error bars on the density come from the uncertainty in the pressure reading. The high density side of these error bars comes from the fact that the minimum vacuum pressure of the chamber was 0.2 mbar, giving a possible residual pressure of air which is 5 times ionized instead of 2 times for helium. The error bars on the period are given by the numerical fit. The solid line corresponds to the period given by the linear theory. We also added on this figure the results of our numerical simulations for two laser energies. As expected for a nonlinear perturbation of cylindrical geometry [13], the plasma period is lower than for a linear perturbation. The measured period decreases such as $n_e^{-1/2}$ and is close to the expected value. We must point out that because of the error bars in the measurements, it is not yet possible to study in detail the nonlinear evolution of the density perturbation. This will be the subject of future experiments.

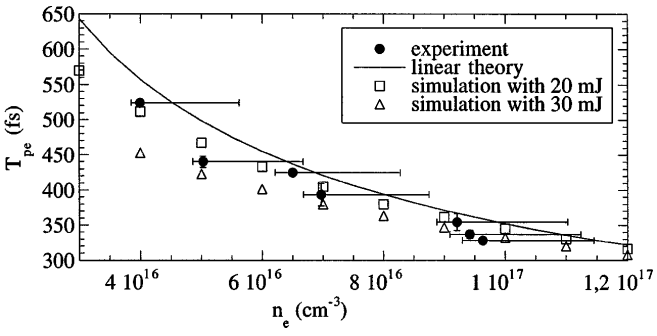

FIG. 5. Electron plasma period versus electron density.

In conclusion, we have presented the first experimental observation of the electron density perturbation produced in a laser pulse wake. The electron oscillation is measured with a time resolution much better than the electron plasma period, and a spatial resolution smaller than the pump focal spot radius. The spatial shape and size of the perturbation agree with the laser wakefield theory. The relative density perturbation amplitude is between 30% and 100%. This amplitude and the measured plasma period are in good agreement with our numerical simulations. We are currently studying in more detail the nonlinear behavior of the electron oscillation and its lifetime.

It is a pleasure to acknowledge help from A. Mysyrowics and G. Rey, and fruitful discussions with P. Mora. This work has been supported by the Centre National de la Recherche Scientifique and by the EU large facility program under Contract No. CHGE CT930021.

[1] T. Tajima and J. M. Dawson, Phys. Rev. Lett. **43**, 267 (1979).
[2] See, e.g., *Advanced Accelerator Concepts*, edited by P. Schoessow, AIP Conf. Proc. No. 335 (AIP, New York, 1995).
[3] S. C. Wilks *et al.*, Phys. Rev. Lett. **62**, 2600 (1989), E. Esarey *et al.*, Phys. Rev. A **42**, 3526 (1990).
[4] Y. Kitagawa *et al.*, Phys. Rev. Lett. **68**, 48 (1992); C. E. Clayton *et al.*, Phys. Rev. Lett. **70**, 37 (1993); N. A. Ebrahim, J. Appl. Phys. **76**, 7645 (1994).
[5] F. Amiranoff *et al.*, Phys. Rev. Lett. **74**, 5220 (1995).
[6] L. M. Gorbunov and V. I. Kirsanov, Sov. Phys. JETP **66**, 290 (1987).
[7] N. E. Andreev *et al.*, Sov. JETP Lett. **55**, 571 (1992); T. M. Antonsen, Jr., and P. Mora, Phys. Rev. Lett. **69**, 2204 (1992); P. Sprangle *et al.*, *ibid.* **69**, 2200 (1992).
[8] A. Modenna *et al.*, Nature (London) **377**, 606 (1995); C. Coverdale *et al.*, Phys. Rev. Lett. **74**, 4659 (1995).
[9] K. Nakajima *et al.*, Phys. Rev. Lett. **74**, 2725 (1995).
[10] H. Hamster *et al.*, Phys. Rev. Lett. **71**, 2725 (1993).
[11] J. P. Geindre *et al.*, Opt. Lett. **19**, 1997 (1994).
[12] S. Augst *et al.*, Phys. Rev. Lett. **63(20)**, 2112 (1989).
[13] J. M. Dawson, Phys. Rev. **113(2)**, 383 (1958).